molecules

MDPI

Communication

Synthesis of Conjugated Tris- and Tetrakis (Carbazolyl) Azulenes with Intense Emission in the Visible Range

Amantay Iskanderov [1], Nurlan Merkhatuly [1,*], Ablaykhan Iskanderov [1], Saltanat Abeuova [2] and Pavel Vojtisek [3]

[1] Laboratory of Organic Semiconductor Chemistry, Karaganda Buketov University, Karaganda 100028, Kazakhstan; org.semicond@yandex.kz (A.I.); aby93@yandex.kz (A.I.)
[2] The Higher School of Natural Sciences, Astana International University, Astana 020000, Kazakhstan; abeuova.salta@gmail.com
[3] Department of Inorganic Chemistry, Charles University, CZ-12800 Praha, Czech Republic
* Correspondence: nurlanmerhatuly@mail.ru

Abstract

New conjugated carbazolyl-substituted azulenes, such as 1,2,3-tris(carbazolyl)azulene and 1,2,3,6-tetrakis(carbazolyl)azulene, were synthesized via cross-coupling reactions in high yields. The resulting compounds exhibit a significant ability to absorb and emit light in the visible region, in the range of 400 to 600 nanometers. Studies have shown that azulene with carbazolyl substituents at positions 1, 2, 3, and 6 possesses unique photophysical properties, manifested as intense emission in the blue photoluminescence region (λ_{PL} at 444 and 490 nm), which is not observed in the original azulene. This feature arises due to the donor properties of carbazolyl substituents, which have a strong effect on the electronic structure of azulene, creating the conditions for a permitted HOMO-LUMO electronic transition.

Keywords: azulene compounds; substituted azulenes; visible absorbances; fluorescent emission; substituted carbazoles; coupling reactions

check for updates

Academic Editor: Cheng Yang

Received: 28 May 2025
Revised: 25 June 2025
Accepted: 26 June 2025
Published: 28 June 2025

Citation: Iskanderov, A.; Merkhatuly, N.; Iskanderov, A.; Abeuova, S.; Vojtisek, P. Synthesis of Conjugated Tris- and Tetrakis (Carbazolyl) Azulenes with Intense Emission in the Visible Range. *Molecules* **2025**, *30*, 2797. https://doi.org/10.3390/molecules30132797

Copyright: © 2025 by the authors. Licensee MDPI, Basel, Switzerland. This article is an open access article distributed under the terms and conditions of the Creative Commons Attribution (CC BY) license (https://creativecommons.org/licenses/by/4.0/).

1. Introduction

The widespread application of aromatic compounds possessing elongated π-electronic systems is due to their crucial role as functional materials in the field of organic optoelectronics.

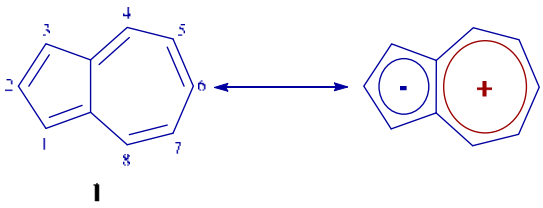
In recent years, increasing attention has been focused on aromatic and heteroaromatic molecules, especially those containing aryl groups or substituents with electron-donor properties. For example, phenylamine naphthalenes and phenylamine anthracenes, due to their pronounced electron donor properties, attract considerable attention from scientists, since they have great potential for use in various fields of organic electronics [1–4].

Their application is considered in such promising areas as the development of organic semiconductors, catalysts for redox reactions, metal-organic frameworks (MOFs), and organic emitting diodes (OLEDs) [5–10].

One of the main advantages of these aromatic systems is their ability to precisely control the electronic structure of materials, which in turn leads to improved performance and optimized morphology.

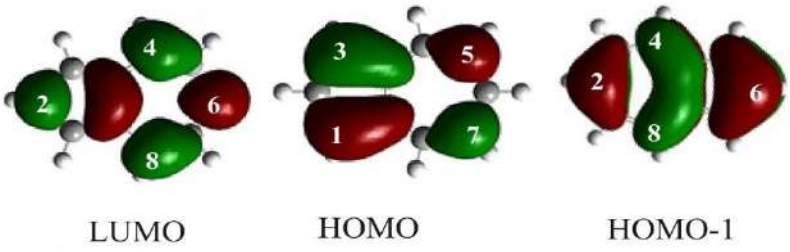
In this regard, it is necessary to emphasize the importance of the structural isomer of naphthalene–azulene [11–20]. Its peculiarity lies in its unique aromatic structure, which determines its unique electronic and optical characteristics. Among them, a polarized structure with a dipole moment of 1.08 D [21] and anomalous fluorescence is particularly noteworthy. This fluorescence deviates from traditional concepts based on Kasha's rule and manifests in a transition between the S_2 and S_0 energy levels [22–24].

Azulene **1** can be represented as a molecule formed by the condensation of the tropylium cation and the cyclopentadiene anion, which is clearly demonstrated in Figure 1a. It is precisely this unique molecular architecture that causes to the deviation of the HOMO and LUMO energy levels from the characteristics typical of standard aromatic hydrocarbons. In the azulene molecule, atoms located at positions 1 and 3, possess large HOMO coefficients, and carbon atoms C_2 and C_6 have large HOMO-1/LUMO (see Figure 1b).



1

(**a**)



(**b**)

Figure 1. (**a**) Structure **1.** (**b**) FMO **1**.

A distinctive feature of azulene **1** compared to naphthalene is its saturated blue color, which indicates the absorption of light corresponding to the transition $S_0 \rightarrow S_1$ (λ max is in the long-wave region of the spectrum at 580 nanometers). However, the molar absorption coefficient has a small value (350 M^{-1} cm^{-1}), which indicates that it does not reach the level expected for the permitted π–π* transition [25].

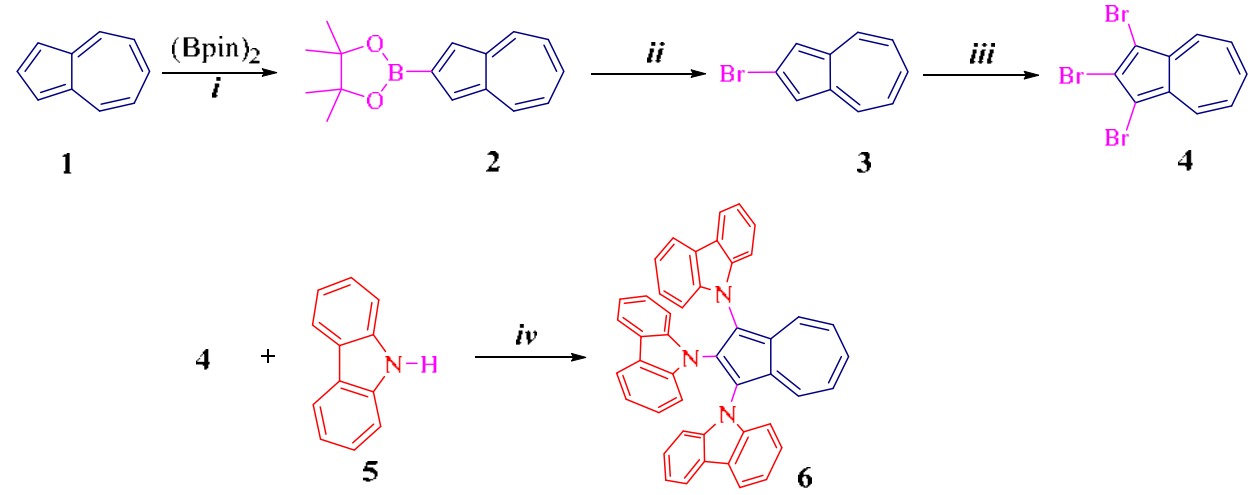
Thus, modification of the structure of azulene by introducing functional groups, especially electron donor groups, can significantly change its electronic properties. This opens up ample opportunities for creating unique materials with unusual optical and electronic characteristics.

In this work, we demonstrate the synthesis of new carbazolyl-substituted azulenes. An effective cross-coupling method yielded 1,2,3-tris(carbazolyl)azulene **6** and 1,2,3,6-tetrakis(carbazolyl)azulene **10** in high yields. The study of photophysical properties of these molecular structures has shown that they lead to an allowed HOMO → LUMO electronic transition. This causes the appearance of intense absorption and luminescence spectra in the visible range.

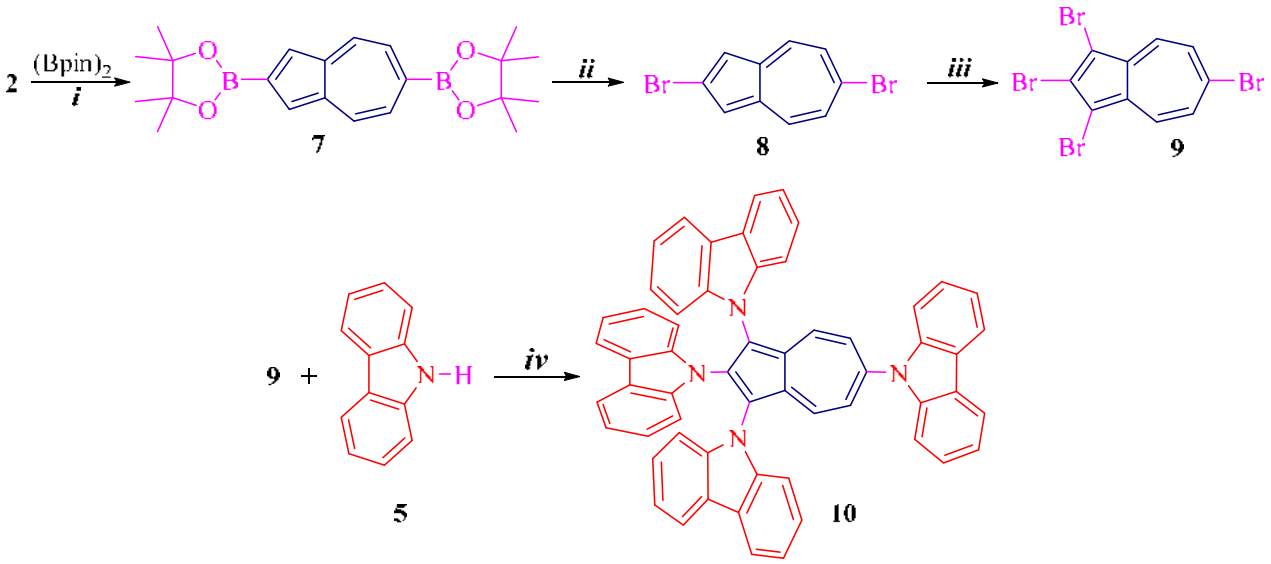
2. Results and Discussions

Schemes 1 and 2 illustrate synthetic routes for azulene conjugated compounds: 1,2,3-tri(carbazolyl)azulene **6** and 1,2,3,6-tetra(carbazolyl)azulene **10.**

As shown (Scheme 1), key molecule **2** was synthesized by direct borylation at the C_2 position of **1** in the presence of an Ir-catalyst, according to the methodology described in the literature [26]. This compound is then successfully reacted with copper bromide to give bromoazulene **3** in 72% yield [27].



Scheme 1. Preparation of **6**: (i) $[Ir(cod)Cl]_2$, 2,2′-bpy, cyclohexane, reflux, 70%; (ii) CuBr, DMF, 90 °C, 72%; (iii) NBS, CH_2Cl_2, −20 °C, 92%; (iv) $Pd(OAc)_2$, *t*-BuOK, *t*-Bu_3PHBF_4, toluene, reflux, 78%.



Scheme 2. Preparation of **10**: (i) $[Ir(cod)Cl]_2$, 2,2′-bpy, cyclohexane, reflux, 50%; (ii) CuBr, DMF, 90 °C, 70%; (iii) NBS, CH_2Cl_2, −20 °C, 90%; (iv) $Pd(OAc)_2$, *t*-BuOK, *t*-Bu_3PHBF_4, toluene, reflux, 75%.

Next, the bromide **3** reacts with NBS (N-bromosuccinimide) to form tribromoazulene **4** in a high yield of 92%. The reaction proceeds regioselectively at the C_1 and C_3 positions.

Finally, the cross-coupling of tribromoazulene **4** and carbazole **5** in toluene, in the presence of a palladium catalyst, gives the final product, tris(carbazolyl)azulene **6**, in a high yield of 78%.

Another key molecule, **7**, was synthesized by selective C_6 borylation of **2** under the above conditions, according to [28] (Scheme 2). Further reaction of diborylazulene **7** with copper bromide gives 2,6-dibromoazulene **8** in 70% yield [27,29]. The resulting dibromide **8** is then also reacted regioselectively at positions 1 and 3 with NBS to give tetrabromoazulene **9** in high yield of 90%. In a similar way, by cross-coupling reaction of tetrabromide **9** and **5**, the final product, tetrakis(carbazolyl)azulene **10**, was obtained. The yield is high, amounting to 75%.

The obtained tris(carbazolyl)azulene **6** and tetrakis(carbazolyl)azulene **10** are colored brown in contrast to the original **1**, which has a blue tint. These compounds are stable solids (Supplementary Materials, Section 3, Figure S13) that are easily soluble in organic solvents (CH_2Cl_2, $CHCl_3$, $C_6H_5CH_3$, and C_6H_5Cl) at ambient temperature.

The structure and purity of synthesized compounds **6** and **10** were proved by NMR (^{1}H and ^{13}C), IR, and Mass spectrometry (Supplementary Materials).

Figure 2 shows the UV-Vis spectra of conjugated tris- and tetrakis(carbazolyl)azulenes **6** and **10**, while Table 1 presents their characteristics.

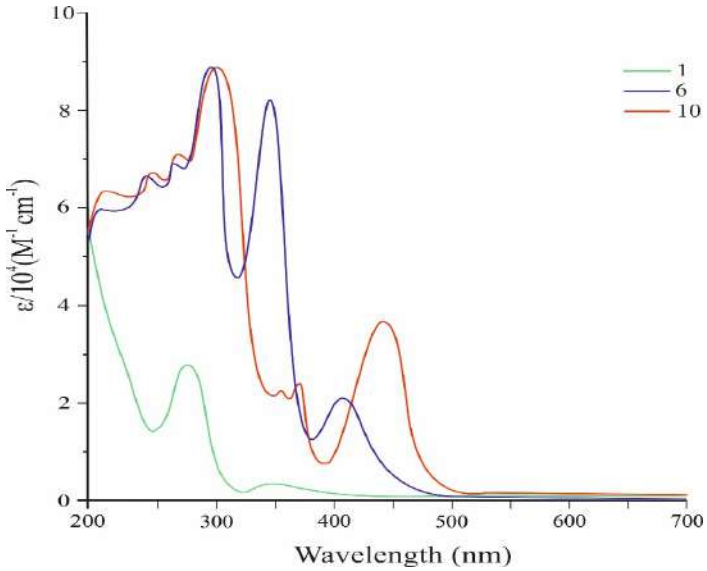


Figure 2. UV–Vis spectra of compounds **6**, **10**, and the original **1**.

Table 1. Photophysical properties of compounds **6** and **10**.

Compound	Absorption [a]		Photoluminescence (PL) [b]					
	λabs (nm)	ε (M^{-1} cm^{-1})	λ_{PL} (nm) [c]	S_1 (eV)	T_1 (eV) [d]	ΔE_{ST} (eV)	τ_p/τ_d (ns/μs) [e]	Φ_{PL} [f]
6	295	88,888	444	3.06	2.79	0.27	7.4/4.6	0.12
	345	82,113						
	407	21,132						
10	267	71,057	490	2.87	2.63	0.24	8.7/19	0.25
	300	88,888						
	441	36,666						

[a] Measured in dichloromethane at room temperature (C = 1 × 10^{-4} M). [b] λ_{ex} (excitation wavelength) 390 nm. [c] Measured in dichloromethane at room temperature. [d] Measured at 77 K dichloromethane. [e] Measured under N_2 in dichloromethane at room temperature. [f] Absolute PLQY measured by integrating sphere under N_2 in dichloromethane at room temperature

The absorption spectra of these compounds were analyzed against the spectrum of the initial molecule **1** (Figure 2).

As shown in Figure 2, the absorption spectrum of the compound **6** in dichloromethane solution shows the appearance of a new visible band with λmax at 407 nm (ε = 21.132 M^{-1} cm^{-1}). The compound **10** also exhibits a strong visible absorption corresponding to the permitted π–π* electron transition with a maximum at 441 nm (ε = 36.666 M^{-1} cm^{-1}).

The effective absorption of visible light in the compounds **6** and **10** is due to the strong electron donor effect of the carbazolyl groups. It should be noted that visible absorbances of **6** and **10** are significantly stronger than that of the original azulene **1**, which has a molar absorption coefficient in the visible region of only 350 M^{-1} cm^{-1} [25].

It is also seen from the spectrum that the visible absorption maximum of **10** is significantly (by 34 nm) shifted to the long-wave region with an increase in intensity compared to the absorption maximum of **6**. These changes may be due to a significant increase in π-conjugation and de-localization of electrons, which leads to narrowing of the HOMO–LUMO gap of molecule **10** (Figure 5).

The study of the electronic absorbances of the compounds **6** and **10** was also carried out in the form of thin films (Supplementary Materials). Analysis of the spectra presented in Figure 3 shows that the absorption pattern of the compounds **6** and **10** in thin films is similar to their absorption in solution (see Figure 3b or Figure 2). However, the visible absorption maxima (λmax at 407 and 441 nm, respectively) for the compounds **6** and **10** are shifted to the long wavelength region by about 13 and 15 nanometers, respectively, compared to the solution. Redshift of spectral bands may be due to intermolecular interaction of compounds in the solid state.

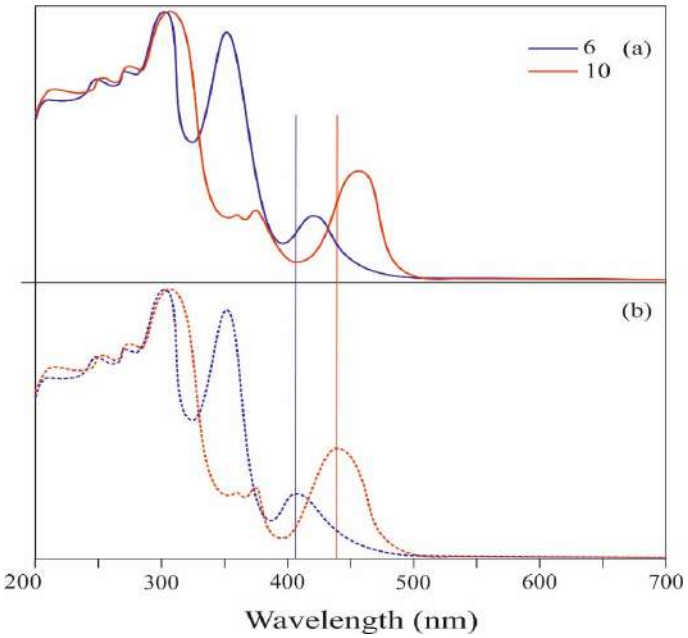


Figure 3. UV–Vis absorption spectra of **6** and **10**: (**a**) in film; (**b**) in CH_2Cl_2.

It is worth noting that the absorption bands of compounds **6** and **10** observed in the spectrum coincide with the wavelength range (380–560 nm) characteristic of commercially available functional materials used in organic solar cells and organic dyes [30–36].

Figure 4 shows the photoluminescence (PL) spectra of tris- and tetrakis (carbazolyl)azulenes **6** and **10** studied in solution, and Table 1 shows their characteristics.

The spectrum shows that compounds **6** and **10** exhibit new photoluminescence bands in the visible region with maxima at 411 and 437 nm. The quantum yields (Φ_{PL}) are 12% and 25%, respectively (Table 1).

The fluorescence spectra of compounds **6** and **10** at room temperature are broad and structureless, while the phosphorescence spectra measured at 77 K show vibrational structures.

The analysis of Table 1 demonstrates that the most donor tetrasubstituted azulene **10** possesses lower S_1 (2.87 eV) and T_1 (2.63 eV) energies compared to the trisubstituted compound **6**. Thus, the S_1 of compound **10** is significantly shifted towards lower energies by 0.19 eV. The T_1 energy also has a shift to lower energies by 0.16 eV. As a result, the ΔE_{ST} of molecule **10** reaches 0.24 eV.

It is also observed that the lifetime (τ_p/τ_d) and the quantum yield of the fluorescence of compound **10** are superior to those of molecule **6** (Table 1).

So, the synthesized carbazolylazulenes **6** and **10** have a significant feature–intense photoluminescence in the visible part of the spectrum, which is not observed in the original azulene **1** [24,25].

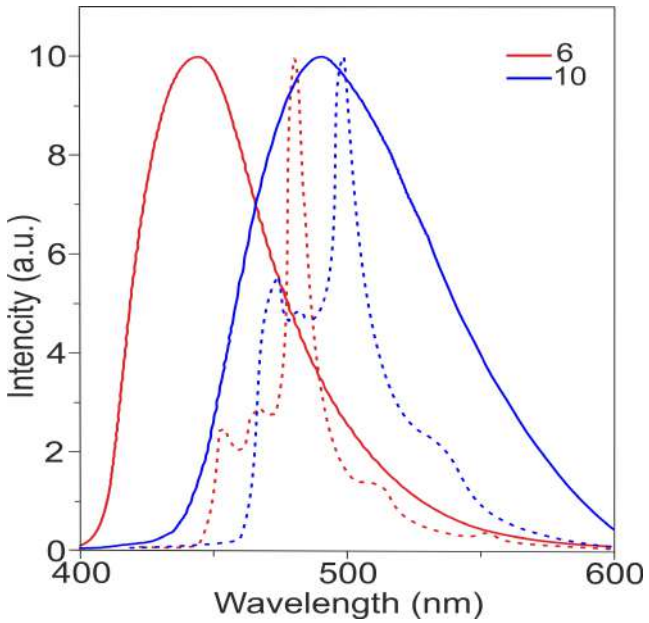


Figure 4. Photoluminescence (PL) spectra of compounds **6** and **10** in dichloromethane. Fluorescence spectra–solid lines, phosphorescence spectra–dashed lines.

Thus, studies of photophysical properties have shown that the introduction of electron-donor carbazolyl groups at positions 1,2,3, and 6 of azulene leads to the appearance of intense electronic absorptions (ε 21.132 M^{-1} cm^{-1} and ε 36.666 M^{-1} cm^{-1}) and unique photoluminescent emissions (Φ_{PL} 12% and 25%) in the visible part of the spectrum.

To understand the electronic properties of the synthesized tris- and tetrakis(carbazolyl) azulenes **6** and **10** and the relationship between their structural configuration and optical behavior, DFT calculations (method B3LYP/6-31G*) were performed (Figure 5, Supplementary Materials).

Figure 5 shows that HOMO (and HOMO-1) of the compounds **6** and **10** are distributed throughout both the azulene structure and at the carbazolyl substituents.

This distribution of orbitals can occur as a result of interaction of HOMO-1 of azulene **1** with HOMO of carbazole **5** [29], because in HOMO of the original azulene C_2 and C_6 are nodal, while in HOMO-1 these atoms are not included in the nodal plane and have large atomic-orbital coefficients (Figure 1b).

Studies also revealed that HOMO (5.25 eV each) and LUMO (−2.44 eV and −2.55 eV) levels of the compounds **6** and **10** occupy lower energy positions compared to similar levels of the original azulene **1.**

At the same time, LUMO levels decrease significantly by 0.61 and 0.72 eV, respectively. As a result, the energy gaps between the frontal orbitals of these compounds narrow by 0.55 eV and 0.66 eV.

Probably, the decrease in FMO causes the permitted π–π* electronic transition in molecules **6** and **10**, in contrast to azulene **1**, where this transition is prohibited [25]. As a result, intense absorption and emission are observed in the visible spectrum (Figures 2 and 4, data in Table 1), which indicates significant differences in the electronic structure of these compounds.

To determine the energy levels of the frontal MO of the carbazolylazulenes **6** and **10**, a CV (cyclic voltammetry) analysis of their redox behavior was carried out (Figure 6, Supplementary Materials).

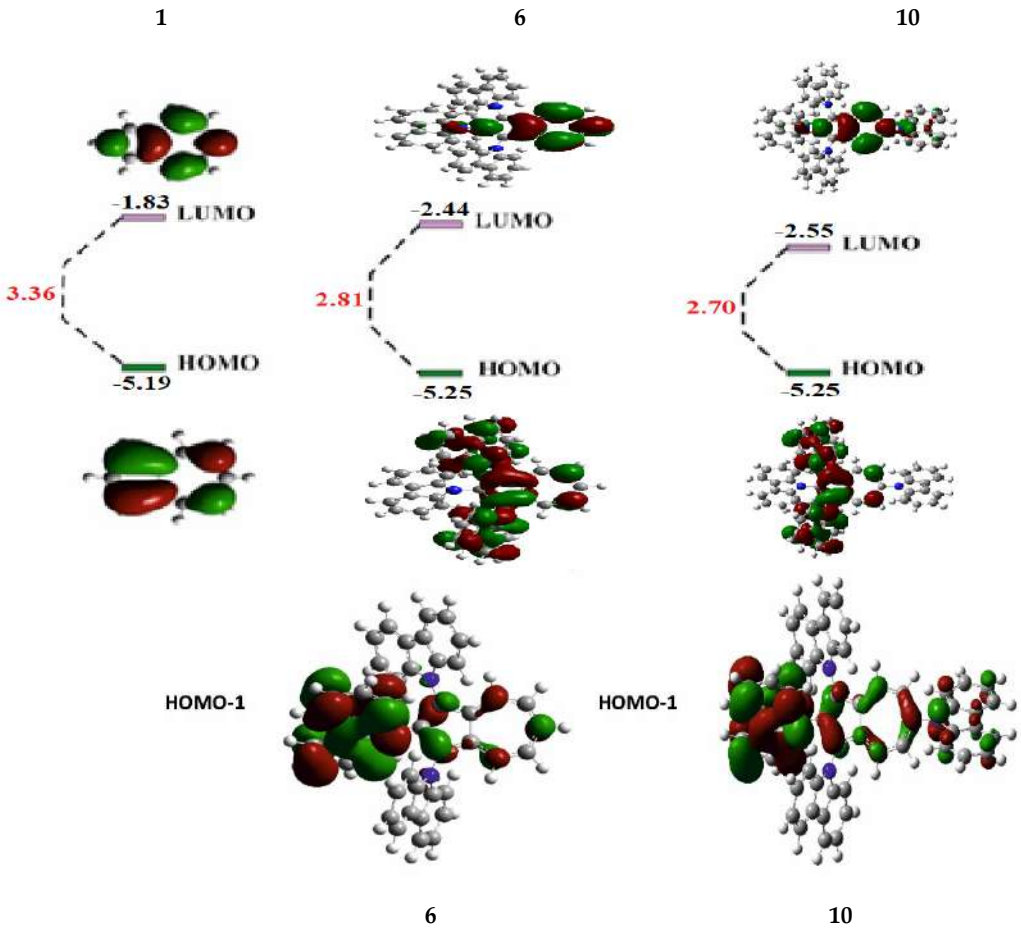
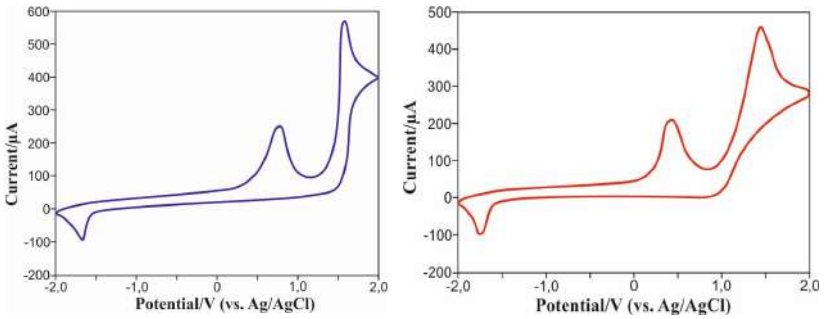


Figure 5. Distribution of frontal MO **6** and **10** versus azulene **1**.



(**a**) (**b**)

Figure 6. Cyclic voltammogram of 6 (**a**) and 10 (**b**).

Analysis of CV curves revealed irreversible double oxidation peaks of the compound **6** at potentials of 0.77 V and 1.58 V. In addition, an irreversible single reduction peak was recorded at a potential of −1.67 V. The compound **10** also exhibited similar behavior, with irreversible oxidation at potentials of 0.43 V and 1.44 V, as well as an irreversible reduction wave observed at −1.75 V. Determining the initial oxidation (0.1 V for Eox^{onset}) and reduction (−1.57 V for $Ered^{onset}$) potentials, we calculated the energy values of the frontal orbitals for the compound **6**: −5.10 eV for HOMO and −2.83 eV for LUMO. Taking into account the initial oxidation (0.08 V for Eox^{onset}) and reduction (–1.50 V for $Ered^{onset}$) potentials, the HOMO and LUMO energy levels for molecule **10** were determined to be −5.12 eV and −2.90 eV, respectively. The calculation of these values was performed on the basis of the formula set forth in [37].

Thus, experimentally determined values of HOMO energy levels for the compounds **6** and **10** demonstrate good consistency with the results obtained using the DFT method. The difference between theoretically calculated and experimentally measured values of LUMO energy levels is insignificant, being approximately 0.39 V and 0.35 V for the compounds **6** and **10**, respectively.

3. Materials and Methods

1,2,3-Tribromoazulene 4. To a solution of monobromazulene **3** (207 mg, 1.00 mmol) in dichloromethane (5 mL) was slowly poured a solution of NBS (389 mg, 2.2 mmol) in dichloromethane (25 mL) at −20 °C under argon and stirred for 1.5 h. Then the mixture was treated with $NaHCO_3$ solution, the organic phase was washed with brine and dried with Na_2SO_4. The resulting solution was filtered through alumina. After concentration on a rotary evaporator and recrystallization from dichloromethane, 337 mg (92%) of a dark green solid was obtained. m.p. 132–133 °C. IR spectrum (ν, cm^{-1}): 2920, 2851, 1581, 1462, 1385, 1269, 725. ^{1}H NMR: δ 7.94 (d, J = 11.4 Hz, $2H^{4,8}{}_{Az}$), 7.62–7.59 (m, $2H^{5,7}{}_{Az}$), 7.33 (t, J = 10.2 Hz, $1H^{6}{}_{Az}$). ^{13}C NMR: δ 139.6, 137.5, 136.3, 135.5, 134.3, 134.2, 128.9, 125.6, 107.1. HRMS (ESI): calcd. for $C_{10}H_5{}^{79}Br_3$ $[M]^+$: 361,7898, found: 361,7891.

1,2,3-Tris(carbazolyl)azulene 6. Tribromoazulene **4** (336 mg, 1.00 mmol) and carbazole **5** (554 mg, 3.6 mmol) were mixed in dry toluene (35 mL) under argon. Palladium (II) acetate (12 mg, 0.05 mmol), *t*-BuOK (941 mg, 16.8 mmol), and *t*-Bu_3PHBF_4 (3.0 mg, 0.01 mmol) were then added. The mixture was then refluxed for 24 h, filtered through Celite and dried with Na_2SO_4. The solvent was removed by rotary evaporation. The pure compound was obtained by purification on silica gel using a 1:9 solution of dichloromethane and hexane (CC with SiO_2) as eluent. After purification, the compound was recrystallized from CH_2CI_2. 487 mg (78%) of a brown solid were obtained. Melting point: 142–143 °C. IR spectrum (ν, cm^{-1}): 2920, 2850, 1583, 1462, 1380, 1269, 724. ^{1}H NMR: δ 8.40 (d, *J* = 9.6 Hz, $2H^{4,8}{}_{Az}$), 8.09–8.03 (m, $6H^{1,8}{}_{Cz}$), 7.91–7.85 (m, $2H^{5,7}{}_{Az}$), 7.62–7.53 (m, $6H^{4,5}{}_{Cz}$,$1H^{6}{}_{Az}$), 7.40–7.33 (m, $12H^{2,3,6,7}{}_{Cz}$). ^{13}C NMR: δ 138.2, 134.8, 134.2, 131.7, 130.8, 126.6, 124.3, 123.6, 123.1, 122.7, 122.2, 118.2, 117.1, 114.9, 112.5. HRMS (ESI): calcd. for $C_{46}H_{29}N_3$ $[M]^+$: 623,0720, found: 623,0712.

1,2,3,6-Tetrabromoazulene 9. To a solution of dibromoazulene **8** (286 mg, 1.00 mmol) in dichloromethane (5 mL) was slowly poured a solution of NBS (389 mg, 2.2 mmol) in dichloromethane (25 mL) at −20 °C under argon. The mixture was then stirred for 2 h. A saturated aqueous solution of sodium hydrogen carbonate was then added, after which the organic layer was separated and washed with brine until neutral. It was then dried over sodium sulfate. The resulting solution was filtered through alumina. Concentration on a rotary evaporator and recrystallization from dichloromethane gave 399 mg (90%) of a dark green solid. Batch 177–178 °C. IR spectrum (ν, cm^{-1}): 2920, 2850, 1580, 1465, 1385, 1269, 725. ^{1}H NMR: δ 8.29 (d, *J* = 9.7 Hz, $2H^{4,8}{}_{Az}$), 7.33 (d, *J* = 9.9 Hz, $2H^{5,7}{}_{Az}$).^{13}C NMR: δ 139.6, 136.3, 135.5, 134,2, 130,9, 129.0, 125.6, 104.7. HRMS (ESI): calcd. for $C_{10}H_4{}^{79}Br_4$ $[M]^+$: 440,0570, found: 440,0563.

1,2,3,6-Tetrakis(carbazolyl)azulene 10. Tetrabromazulene **9** (444 mg, 1.00 mmol) and carbazole 5 (738 mg, 4.8 mmol) were mixed in dry toluene (45 mL). The catalyst palladium (II) acetate (12 mg, 0.05 mmol), *t*-BuOK (1.254 g, 22.4 mmol), and *t*-Bu_3PHBF_4 (3.0 mg, 0.01 mmol) were then added to the mixture under continuous argon purge at ambient conditions. The mixture was then refluxed for 24 h, filtered through Celite and dried over sodium sulfate. The solvent was removed by rotary evaporation. The pure compound was obtained by purification on silica gel using a 1:9 solution of DCM and hexane (CC with SiO_2) as eluent. After purification, the compound was recrystallized from CH_2Cl_2. 590 mg (75%) of a dark brown solid was obtained. Melting point: 146–148 °C. IR spectrum (ν, cm^{-1}): 2920,

2854, 1580, 1461, 1384, 1268, 725. ^{1}H NMR: δ 8.40 (d, J = 11.6 Hz, 2H$^{4,8}{}_{Az}$), 8.22–8.20 (m, 8H$^{1,8}{}_{Cz}$), 7.63–7.57 (m, 2H$^{5,7}{}_{Az}$),7.37–7.31 (m, 8H$^{4,5}{}_{Cz}$), 6.92–6.90 (m, 16H$^{2,3,6,7}{}_{Cz}$). ^{13}C NMR: δ 139.9, 135.4, 134.4, 126,7, 126,6, 124.5, 124.3, 122.09, 122.06, 122.05, 121.4, 121.3, 120.7, 120.7, 110.1, 109.2, 106.6. HRMS (ESI): calcd. for $C_{58}H_{36}N_4$ $[M]^+$: 788,0685, found: 788,0678.

4. Conclusions

The synthesis of tris- and tetrakis(carbazolyl)azulenes **6** and **10** in high yields and their subsequent careful analysis showed that these compounds possess special optical characteristics. The inclusion of carbazolyl groups at positions 1,2,3, and 6 of azulene leads to pronounced absorbing and emitting properties in the visible spectrum (400–600 nm), in particular to intense emission in the region in the blue region, which is not demonstrated by the compound **1**. DFT calculations support these results by showing changes in the electronic structure that make possible $\pi \rightarrow \pi^*$ electronic transitions previously qualified as prohibited. These conjugated compounds have great potential for applications in organic optoelectronics and materials science.

Supplementary Materials: The following supporting information can be downloaded at: https://www.mdpi.com/article/10.3390/molecules30132797/s1, Figure S1: ^{1}H NMR spectra of 1,2,3-tribromoazulene **4**.; Figure S2: ^{13}C NMR spectra of 1,2,3-tribromoazulene **4**; Figure S3: HRMS spectra of 1,2,3-tribromoazulene **4**; Figure S4: ^{1}H NMR spectra of 1,2,3-tris(carbazolyl)azulene **6**; Figure S5: ^{13}C NMR spectra of 1,2,3-tris(carbazolyl)azulene 6; Figure S6: ^{13}C NMR spectra of 1,2,3,6-tetrabromoazulene **9**; Figure S7: ^{1}H NMR spectra of 1,2,3,6-tetrakis(carbazolyl)azulene **10**; Figure S8: ^{13}C NMR spectra of 1,2,3,6-tetrakis(carbazolyl)azulene **10**; Figure S9: HRMS spectra of 1,2,3,6-tetrabromoazulene **9**; Figure S10: ^{1}H NMR spectra of 1,2,3,6-tetrakis(carbazolyl)azulene **10**; Figure S11: ^{13}C NMR spectra of 1,2,3,6-tetrakis(carbazolyl)azulene **10**; Figure S12: HRMS spectra of 1,2,3,6-tetrakis(carbazolyl)azulene **10**; Figure S13: Thermogravimetric (TGA) analysis of carbazolylazulene **6** and **10;** Table S1: Atomic coordinates of optimized geometry of **6**; Table S2: Atomic coordinates of optimized geometry of **10**.

Author Contributions: Conceptualization, N.M.; methodology, N.M.; software, A.I. (Amantay Iskanderov) and A.I. (Ablaykhan Iskanderov); validation, N.M., A.I. (Amantay Iskanderov), A.I. (Ablaykhan Iskanderov) and S.A.; formal analysis, A.I. (Amantay Iskanderov) and A.I. (Ablaykhan Iskanderov); investigation, N.M., A.I. (Amantay Iskanderov) and A.I. (Ablaykhan Iskanderov); resources, N.M.; data curation, N.M., A.I. (Amantay Iskanderov) and A.I. (Ablaykhan Iskanderov), S.A. and P.V.; writing—original draft preparation, N.M.; writing—review and editing, N.M.; visualization, A.I. (Amantay Iskanderov), A.I. (Ablaykhan Iskanderov), S.A. and P.V.; supervision, N.M. and S.A.; project administration, N.M. All authors have read and agreed to the published version of the manuscript.

Funding: This research is funded by the Committee of Science of the Ministry of Science and Higher Education of the Republic of Kazakhstan (Grant No. BR21882309).

Institutional Review Board Statement: Not applicable.

Informed Consent Statement: Not applicable.

Data Availability Statement: Not applicable.

Conflicts of Interest: The authors declare no conflicts of interest.

References

1. Wu, C.; Djurovich, P.I.; Thompson, M.E. Study of energy transfer and triplet exciton diffusion in hole-transporting host materials. *Adv. Funct. Mater.* **2009**, *19*, 3157–3164. [CrossRef]
2. Taniguchi, R.; Noto, N.; Tanaka, S.; Takahashi, K.; Sarkar, S.K.; Oyama, R.; Abe, M.; Koike, T.; Akita, M. Simple generation of various α-monofluoroalkyl radicals by organic photoredox catalysis: Modular synthesis of β-monofluoroketones. *Chem. Commun.* **2021**, *57*, 2609–2612. [CrossRef]

3. Noto, N.; Koike, T.; Akita, M. Visible-Light-Triggered Monofluoromethylation of Alkenes by Strongly Reducing 1,4-Bis(diphenylamino)naphthalene Photoredox Catalysis. *ACS Catal.* **2019**, *9*, 4382–4387. [CrossRef]
4. Wang, X.; Zhang, Z.; Song, Y.; Su, Y.; Wang, X. Bis(phenothiazine)arene diradicaloids: Isolation, characterization and crystal structures. *Chem. Commun.* **2015**, *51*, 11822–11825. [CrossRef]
5. Freudenberg, J.; Jänsch, D.; Hinkel, F.; Bunz, U.H.F. Immobilization Strategies for Organic Semiconducting Conjugated Polymers. *Chem. Rev.* **2018**, *118*, 5598–5689. [CrossRef]
6. Roy, M.; Walton, J.H.; Fettinger, J.C.; Balch, A.L. Direct Crystallization of Diamine Radical Cations: Carbon-Nitrogen Bond Formation from the Reaction of Triphenylamine with $TiCl_4$, $TiBr_4$,or $SnCl_4$ versus Carbon-Carbon Bond Formation with $SbCl_5$. *Chem.–Eur. J.* **2022**, *28*, e202104631. [CrossRef]
7. Zhang, J.; Chen, Z.; Yang, L.; Pan, F.-F.; Yu, G.-A.; Yin, J.; Liu, S.H. Elaborately Tuning Intramolecular Electron Transfer Through Varying Oligoacene Linkers in the Bis(diarylamino) Systems. *Sci. Rep.* **2016**, *6*, 36310. [CrossRef] [PubMed]
8. Wang, G.; Dmitrieva, E.; Kohn, B.; Scheler, U.; Liu, Y.; Tkachova, V.; Yang, L.; Fu, Y.; Ma, J.; Zhang, P. An Efficient Rechargeable Aluminum–Amine Battery Working Under Quaternization Chemistry. *Angew. Chem. Int. Ed.* **2022**, *61*, e202116194. [CrossRef]
9. Chen, Y.; Gao, X.; Johnson, L.R.; Bruce, P.G. Kinetics of lithium peroxide oxidation by redox mediators and consequences for the lithium–oxygen cell. *Nat. Commun.* **2018**, *9*, 767. [CrossRef]
10. Mayer, D.C.; Manzi, A.; Medishetty, R.; Winkler, B.; Schneider, C.; Kieslich, G.; Pöthig, A.; Feldmann, J.; Fischer, R.A. Controlling Multiphoton Absorption Efficiency by Chromophore Packing in Metal-Organic Frameworks. *J. Am. Chem. Soc.* **2019**, *141*, 11594–11602. [CrossRef]
11. Tsuchiya, T.; Higashibeppu, M.; Mazaki, Y. Synthesis and Properties of Twisted and Helical Azulene Oligomers and Azulene-Based Polycyclic Hydrocarbons. *ChemistryOpen* **2023**, *12*, e202100298. [CrossRef] [PubMed]
12. Tsuchiya, T.; Katsuoka, Y.; Yoza, K.; Sato, H.; Mazaki, Y. Stereochemistry, Stereodynamics, and Redox and Complexation Behaviors of 2,2′-Diaryl-1,1′-Biazulenes. *ChemPlusChem* **2019**, *84*, 1659–1667. [CrossRef]
13. Tsuchiya, T.; Umemura, R.; Kaminaga, M.; Kushida, S.; Ohkubo, K.; Noro, S.I.; Mazaki, Y. Paddlewheel Complexes with Azulenes:Electronic Interaction between Metal Centers and Equatorial Ligands. *ChemPlusChem* **2019**, *84*, 655–664. [CrossRef] [PubMed]
14. Konishi, A.; Yasuda, M. Breathing new life into nonalternant hydrocarbon chemistry: Syntheses and properties of polycyclic hydrocarbons containing azulene, pentalene, and heptalene frameworks. *Chem. Lett.* **2021**, *50*, 195–212. [CrossRef]
15. Xin, H.; Hou, B.; Gao, X. Azulene-Based π-Functional Materials: Design, Synthesis, and Applications. *Acc. Chem. Res.* **2021**, *54*, 1737–1753. [CrossRef]
16. Elwahy, A.H.; Hafner, K. Alkynylazulenes as Building Blocks for Highly Unsaturated Scaffolds. *Asian J. Org. Chem.* **2021**, *10*, 2010–2083. [CrossRef]
17. Bakun, P.; Czarczynska-Goslinska, B.; Goslinski, T.; Lijewski, S. In vitro and in vivo biological activities of azulene derivatives with potential applications in medicine. *Med. Chem. Res.* **2021**, *30*, 834–846. [CrossRef]
18. Lvov, A.G.; Bredihhin, A. Azulene as an ingredient for visible-light- and stimuli-responsive photo switches. *Org. Biomol. Chem.* **2021**, *19*, 4460–4468. [CrossRef]
19. Murfin, L.C.; Lewis, S.E. Azulene—A Bright Core for Sensing and Imaging. *Molecules* **2021**, *26*, 353. [CrossRef]
20. Shoji, T.; Ito, S.; Yasunami, M. Synthesis of Azulene Derivatives from 2H-Cyclohepta[b]furan-2-ones as Starting Materials: Their Reactivity and Properties. *Int. J. Mol. Sci.* **2021**, *22*, 10686. [CrossRef]
21. Anderson, A.G.; Steckler, B.M. Azulene. VIII. A Study of the Visible Absorption Spectra and Dipole Moments of Some 1- and 1,3-Substituted Azulenes. *J. Am. Chem. Soc.* **1959**, *81*, 4941–4946. [CrossRef]
22. Del Valle, J.C.; Catalán, J. A Reappraisal of Kasha's Rule. *Phys. Chem. Chem. Phys.* **2019**, *21*, 10061–10069. [CrossRef]
23. Behera, S.K.; Park, S.Y.; Gierschner, J. Dual Emission: Classes, Mechanisms, and Conditions. *Angew. Chem. Int. Ed.* **2021**, *60*, 22624–22638. [CrossRef]
24. Dunlop, D.; Ludvíková, L.; Banerjee, A.; Ottosson, H.; Slanina, T. Excited-State (Anti)Aromaticity Explains Why Azulene Disobeys Kasha's Rule. *J. Am. Chem. Soc.* **2023**, *145*, 21569–21575. [CrossRef]
25. Shevyakov, S.V.; Li, H.; Muthyala, R.; Asato, A.E.; Croney, J.C.; Jameson, D.M.; Liu, R.S. Orbital control of the color and excited state properties of formylated and fluorinated derivatives of azulene. *J. Phys. Chem. A* **2003**, *107*, 3295–3299. [CrossRef]
26. Kurotobi, K.; Miyauchi, M.; Takakura, K.; Murafuji, T.; Sugihara, Y. Direct Introduction of a Boryl Substituent into the 2-Position of Azulene: Application of the Miyaura and Smith Methods to Azulene. *Eur. J. Org. Chem.* **2003**, *2003*, 3663–3665. [CrossRef]
27. Narita, M.; Murafuji, T.; Yamashita, S.; Fujinaga, M.; Hiyama, K.; Oka, Y.; Tani, F.; Kamijo, S.; Ishiguro, K. Synthesis of 2-Iodoazulenes by the Iododeboronation of Azulen-2-ylboronic Acid Pinacol Esters with Copper(I) Iodide. *J. Org. Chem.* **2018**, *83*, 1298–1303. [CrossRef] [PubMed]
28. Fujinaga, M.; Murafuji, T.; Kurotobi, K.; Sugihara, Y. Polyborylation of azulenes. *Tetrahedron* **2009**, *65*, 7115–7121. [CrossRef]
29. Tsuchiya, T.; Hamano, T.; Inoue, M.; Nakamura, T.; Wakamiya, A.; Mazaki, Y. Intense absorption of azulene realized by molecular orbital inversion. *Chem. Commun.* **2023**, *59*, 10604–10607. [CrossRef]

30. Rahimi, K.; Botiz, I.; Agumba, J.O.; Motamen, S.; Stingelin, N.; Reiter, G. Light absorption of poly(3-hexylthiophene) single crystals. *RSC Adv.* **2014**, *4*, 11121–11123. [CrossRef]
31. Wang, Z.-S.; Koumura, N.; Cui, Y.; Takahashi, M.; Sekiguchi, H.; Mori, A.; Kubo, T.; Furube, A.; Hara, K. Hexylthiophene-Functionalized Carbazole Dyes for Efficient Molecular Photovoltaics: Tuning of Solar-Cell Performance by Structural Modification. *Chem. Mater.* **2008**, *20*, 3993–4003. [CrossRef]
32. Shirota, Y.; Kageyama, H. Charge Carrier Transporting Molecular Materials and Their Applications in Devices. *Chem. Rev.* **2007**, *107*, 953–1010. [CrossRef] [PubMed]
33. Ren, S.; Habibi, A.; Ni, P.; Nahdi, H.; Bouanis, F.Z.; Bourcier, S.; Clavier, G.; Frigoli, M.; Yassar, A. Synthesis and characterization of solution-processed indophenine derivatives for function as a hole transport layer for perovskite solar cells. *Dye. Pigment.* **2023**, *213*, 111136. [CrossRef]
34. Ren, S.; Wang, Z.; Zhang, W.; Ding, Y.; Yi, Z. Donor-acceptor-based organic polymer semiconductor materials to achieve high hole mobility in organic field-effect transistors. *Polymers* **2023**, *15*, 3713. [CrossRef]
35. Murphy, A.R.; Fréchet, J.M.J. Organic Semiconducting Oligomers for Use in Thin Film Transistors. *Chem. Rev.* **2007**, *107*, 1066–1096. [CrossRef]
36. Zaumseil, J.; Sirringhaus, H. Electron and Ambipolar Transport in Organic Field-Effect Transistors. *Chem. Rev.* **2007**, *107*, 1296–1323. [CrossRef]
37. Ren, S.; Wang, Z.; Zhang, W.; Yassar, A.; Chen, J.; Wang, S. Incorporation of diketopyrrolopyrrole into polythiophene for the preparation of organic polymer transistors. *Molecules* **2024**, *29*, 260. [CrossRef]

Disclaimer/Publisher's Note: The statements, opinions and data contained in all publications are solely those of the individual author(s) and contributor(s) and not of MDPI and/or the editor(s). MDPI and/or the editor(s) disclaim responsibility for any injury to people or property resulting from any ideas, methods, instructions or products referred to in the content.